JACS
JOURNAL OF THE AMERICAN CHEMICAL SOCIETY
Article
pubs.acs.org/JACS

Thermal Stability of $Li_2B_{12}H_{12}$ and its Role in the Decomposition of $LiBH_4$

Mark P. Pitt,*[†] Mark Paskevicius,[†] David H. Brown,[‡] Drew A. Sheppard,[†] and Craig E. Buckley[†]

[†]Department of Imaging and Applied Physics, Fuels and Energy Technology Institute, Curtin University, GPO Box U1987, Perth 6845, WA, Australia

[‡]Department of Chemistry, Curtin University, Kent Street, Bentley 6102 WA, Australia

Supporting Information

ABSTRACT: The purpose of this study is to compare the thermal and structural stability of single phase $Li_2B_{12}H_{12}$ with the decomposition process of $LiBH_4$. We have utilized differential thermal analysis/thermogravimetry (DTA/TGA) and temperature programmed desorption-mass spectroscopy (TPD-MS) in combination with X-ray diffraction (XRD) and Fourier transform infrared (FTIR) spectroscopy to study the decomposition products of both $LiBH_4$ and $Li_2B_{12}H_{12}$ up to 600 °C, under both vacuum and hydrogen (H_2) backpressure. We have synthesized highly pure single phase crystalline anhydrous $Li_2B_{12}H_{12}$ (*Pa*-3 structure type) and studied its sensitivity to water and the process of deliquescence. Under either vacuum or H_2 backpressure, after 250 °C, anhydrous $Li_2B_{12}H_{12}$ begins to decompose to a substoichiometric $Li_2B_{12}H_{12-x}$ composition, which displays a very broad diffraction halo in the *d*-spacing range 5.85−7.00 Å, dependent on the amount of H released. Aging *Pa*-3 $Li_2B_{12}H_{12}$ under 450 °C/125 bar H_2 pressure for 24 h produces a previously unobserved well-crystallized β-$Li_2B_{12}H_{12}$ polymorph, and a nanocrystalline γ-$Li_2B_{12}H_{12}$ polymorph. The isothermal release of hydrogen pressure from $LiBH_4$ along the plateau and above the melting point (T_m = 280 °C) initially results in the formation of LiH and γ-$Li_2B_{12}H_{12}$. The γ-$Li_2B_{12}H_{12}$ polymorph then decomposes to a substoichiometric $Li_2B_{12}H_{12-x}$ composition. The *Pa*-3 $Li_2B_{12}H_{12}$ phase is not observed during $LiBH_4$ decomposition. Decomposition of $LiBH_4$ under vacuum to 600 °C produces LiH and amorphous B with some Li dissolved within it. The lack of an obvious B−Li−B or B−H−B bridging band in the FTIR data for $Li_2B_{12}H_{12-x}$ suggests the H poor $B_{12}H_{12-x}$ pseudo-icosahedra remain isolated and are not polymerized. $Li_2B_{12}H_{12-x}$ is persistent to at least 600 °C under vacuum, with no LiH formation observable and only a ca. *d* = 7.00 Å halo remaining. By 650 °C, $Li_2B_{12}H_{12-x}$ is finally decomposed, and amorphous B can be observed, with no LiH reflections. Further studies are required to clarify the structural symmetry of the β- and γ-$Li_2B_{12}H_{12}$ polymorphs and substoichiometric $Li_2B_{12}H_{12-x}$.

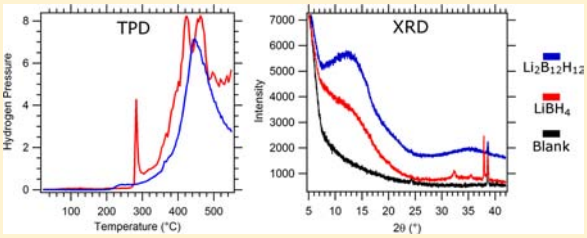

1. INTRODUCTION

Metal−hydrogen systems containing boron have garnered great scientific interest recently due to their intrinsically high gravimetric and volumetric densities, placing them in an ideal position for stationary and vehicular hydrogen-based power systems. Tetravalent complex borohydride phases, such as $LiBH_4$ and $Mg(BH_4)_2$, contain a remarkable 18.5 and 14.9 wt % H, respectively. Studies on the hydrogen release and uptake of decomposed products of these phases have shown intrinsically high temperatures (>T_m, melting temperature) to both release and reabsorb hydrogen for $LiBH_4$[1−7] and $Mg(BH_4)_2$.[8−10] Minor amounts of catalytic phases (generally containing transition metals in the form of salts or nanoparticulate alloys) have little effect in reducing the reabsorption temperature (>T_m) for tetravalent borohydrides, demonstrating the BH_4^- tetrahedral unit possesses stable B−H bonding, which can survive well past T_m in the molten state, dependent on hydrogen backpressure.[11,12] Decomposition studies of metal-borohydrides milled with additives typically erroneously assume a catalytic effect when, for example, $LiBH_4$ reacts with the additive, irreversibly consuming the hydride into segregated nonhydrogen reversible products.[13] The need for high temperatures > T_m stands in stark contrast to Al-containing complex hydrides, such as $NaAlH_4$, where the presence of minor amounts of early transition metals, such as Ti, allows hydrogen reversibility below T_m and significant lengthening/breaking of Al−H bonds at the near surface transition-metal/hydride interface.[14] As such, decomposition studies of pure tetravalent borohydride phases typically proceed well past T_m to allow hydrogen release and reveal complex multiple-phase transitions for temperatures >T_m.[15] For example, in situ diffraction studies of the $Mg(BH_4)_2$ decomposition process above T_m have only recently revealed intense and broad high *d*-spacing diffraction halos that are representative of the dominant boron-containing phase(s),[15] with the only obvious sharp crystalline reflections from MgH_2 and at the final stages of H release, MgB_2. Similarly for decomposed $LiBH_4$ samples, LiH is typically the only well-crystallized phase observed by diffraction.[2−5] Due to the broad nature of the halos, structural

Received: January 6, 2013
Published: April 12, 2013

   dx.doi.org/10.1021/ja400131b | *J. Am. Chem. Soc.* 2013, 135, 6930−6941

identification of the boron-containing phases(s) in postmelted borohydride samples by diffraction is difficult, and studies resorted to spectroscopic techniques, such as solid-state ^{11}B nuclear magnetic resonance (NMR) and Raman/FTIR spectroscopy. In particular, solid-state ^{11}B NMR studies have consistently interpreted the appearance of a signal in the −12 to −15 ppm range in decomposed $LiBH_4$[16] and $Mg(BH_4)_2$,[16,17] as an indication of the formation of $B_{12}H_{12}^{2-}$ containing species, such as $Li_2B_{12}H_{12}$ and $MgB_{12}H_{12}$, during decomposition past T_m. This interpretation is corroborated by the presence of strong B−H stretching bands in the 2500 cm^{-1} region of Raman spectra.[3,18−20] However, for decomposed $Mg(BH_4)_2$, this NMR analysis is in conflict with: (i) the position in *d*-spacing of the broad diffraction halo occurs significantly higher than the strongest reflection of the proposed crystalline $MgB_{12}H_{12}$ structure;[19] (ii) the ex-situ weight standard quantification of the average Mg−B−H composition of the high *d*-spacing halo gives an average composition that cannot be reproduced by phases proposed from solid-state ^{11}B NMR data; and (iii) the presence of bridging bands and lower than expected magnitudes of B−H stretches[15] that would be different to pure $MgB_{12}H_{12}$. These conflicts suggest that the interpretation of ^{11}B NMR data by itself is misleading, consistent with the ca. −15 ppm chemical shift for decomposed $Mg(BH_4)_2$ samples moving downfield by ca. +8 ppm from ca. 320−370 °C.[17] Commensurate with this +8 ppm shift is H release from the sample and verifiable color changes of the decomposed powder as the MgH_2 fraction increases, showing Mg loss from the high *d*-spacing boron-containing phase(s).[15] Attempts to explain point (i) by $MgB_{12}H_{12}$ being amorphous are spurious, as such a phase has never been observed by any experimental technique, similarly for $Li_2B_{12}H_{12}$.

With the novel observation and quantification of high *d*-spacing diffraction halos for decomposed $Mg(BH_4)_2$ samples producing different interpretations to ^{11}B NMR data, a reinvestigation of the decomposition of $LiBH_4$ is warranted. The major difference in this case is that anhydrous $Li_2B_{12}H_{12}$ can be synthesized in single phase form, while $MgB_{12}H_{12}$ is yet to be.[21] This allows independent structural verification for the proposed decomposition products of $LiBH_4$. While anhydrous crystalline $Li_2B_{12}H_{12}$ is structurally well characterized,[22] studies on the stability of $Li_2B_{12}H_{12}$ in relation to decomposed $LiBH_4$ are surprisingly sparse. Diffraction studies of decomposed $LiBH_4$ samples generally do not collect data to low enough angles to discern potential $B_{12}H_{12}$-containing phases, and there exists only one study in the literature revealing a high *d*-spacing halo for decomposed $LiBH_4$ samples. However, the presence of this high *d*-spacing halo in the data was not discussed.[5] Recent studies of decomposed $LiBH_4$[7] have indicated that its decomposition products (proposed as $Li_2B_{12}H_{12}$ or adducts thereof) are stable up to 600 °C/10 bar, based on the B−H stretching bands observed in $LiBH_4$ decomposition products and solid-state ^{11}B NMR data. Further, there are indications that loss of ca. 2 H atoms from single phase "well dehydrated" $Li_2B_{12}H_{12}$ occurs by 450 °C, with an associated shift of the signal in the ^{11}B NMR spectrum to ca. −12 ppm.[23] Early studies of the thermal stability of group I metal-$B_{12}H_{12}$ single phase systems demonstrated an increasing trend of stability from Li to Cs,[24] with extreme stability evident for Cs, reported to be recovered at 800 °C unchanged.[25] Minor outgassing in the 600−650 °C range accompanied by exothermic spikes was evident for Cs, however, the gas was not identified.[26] In contrast, more recent studies[27] of $Cs_2B_{12}H_{12}$ thermal decomposition under Ar demonstrates that unidentified mass loss does occur at ca. 400 °C before massive weight loss at ca. 900 °C, attributable to loss of all Cs from the sample. Mass losses in other systems, such as K[28] and Na,[29] could be related to the loss of water, and as discussed for the review of metal-$B_{12}H_{12}$ salts,[30] mass losses during thermal treatment have not been unambiguously assigned to either water, hydrogen, or potentially a combination of both. For the group II case of Ca, the loss of ca. 2.4 H atoms from anhydrous $CaB_{12}H_{12}$ can be observed by 600 °C.[31]

Currently, the literature concerning the decomposition of metal-$B_{12}H_{12}$ salts is sparse and ambiguous in terms of temperature differences in the order of several hundred degrees. The exact thermal stability range of $Li_2B_{12}H_{12}$ is not clear, which can be directly attributed to the synthesis of the phase and removal of water/adducts from it and the potential loss of H and Li at higher temperatures. As such, the thermal stability of $Li_2B_{12}H_{12}$ is currently ambiguous and open to interpretation with regard to its proposed stability range in decomposed $LiBH_4$.[7,32,33]

In this study, we carefully follow the temperature-dependent structural stability of $Li_2B_{12}H_{12}$ under vacuum and hydrogen backpressure well beyond T_m of $LiBH_4$. Our findings strongly support the notion that solid-state ^{11}B NMR data have often been structurally misinterpreted, and that $Li_2B_{12}H_{12-x}$ compositions are the intermediate compounds during $LiBH_4$ decomposition.

2. EXPERIMENTAL SECTION

$LiBH_4$ (batch no. 21898PJ, 97.4% purity) was obtained from Sigma-Aldrich. $(Et_3NH)_2(B_{12}H_{12})$ was prepared following literature procedure[34] using decaborane (ca. 5 g, Alfa Aesar), triethylamine-borane (ca. 12 mL, Sigma-Aldrich), and hexadecane as the solvent. $Li_2B_{12}H_{12}{\cdot}xH_2O$:lithium hydroxide hydrate (1.1 g, 26 mmol) was added portionwise to a stirred suspension of $(Et_3NH)_2(B_{12}H_{12})$ (3.49 g, 10 mmol) in water (ca. 150 mL) in a PTFE beaker, under a blanket of nitrogen. The mixture was then heated at ca. 80 °C under a nitrogen stream until dry. The solid residue was dissolved in water (40 mL), Amberlite-IRC86 (H form) (ca. 10 mL wet bead volume) was added, and the mixture was stirred at room temperature for 1 h. The aqueous phase tested neutral by indicator paper. The mixture was filtered, and the filtrate concentrated to dryness by heating at ca. 90 °C under a stream of nitrogen and then under high vacuum at room temperature to afford a white powder (2.37 g). ^{1}H NMR (D_2O): δ 0.5−1.8 (m); ^{11}B NMR (D_2O): −15.4 (d, J = 126 Hz). ^{1}H and ^{11}B NMR spectra were recorded on a Bruker AVN400 NMR spectrometer (400.1 MHz for ^{1}H; 128.4 for ^{11}B). ^{11}B NMR spectra were referenced to an external solution of $Et_2O{\cdot}BF_3$ in $CDCl_3$.

After synthesis, $Li_2B_{12}H_{12}{\cdot}xH_2O$ and its products were handled in an inert argon glovebox to prevent air exposure (<1 ppm O_2 and H_2O). $Li_2B_{12}H_{12}{\cdot}xH_2O$ was dehydrated to $Li_2B_{12}H_{12}$ by thermal treatment at 225 °C in an airtight, flow-through vessel for up to 6 h under He (99.999%) flow (2 L/min).

To test for amorphization, ball milling of $Li_2B_{12}H_{12}$ was performed in an Across International PQ-N04 planetary mill using a 50 mL stainless steel 304 vial and 10 mm balls, at 400 rpm with a ball to powder ration of 20:1.

X-ray Diffraction (XRD) data were collected using a Bruker D8 Advance diffractometer (Cu−Kα_{1+2} radiation, λ = 1.54 Å). The instrument is equipped with a LynxEye linear position sensitive detector (PSD) with 192 pixels over 3° 2θ. The instrumental line broadening of the Bruker D8 is modeled utilizing a NIST 660a LaB_6 reference standard ($\Delta d/d \sim 5.3 \times 10^{-4}$). Samples were enclosed within an airtight poly(methyl methacrylate) bubble holder or under an Al film to prevent air exposure during data collection. All samples

dx.doi.org/10.1021/ja400131b | J. Am. Chem. Soc. 2013, 135, 6930−6941

were measured on a single crystal Si wafer to eliminate the presence of broad diffraction halos that can occur from some sample holders, such as glass. Diffraction patterns were analyzed with the Rietveld method using TOPAS (Bruker-AXS). NIST 660a LaB_6 was also used as an internal line shape and weight quantification standard.

Differential thermal analysis with thermogravimetric analysis (DTA/TGA) was performed on a TA Instruments SDT-Q600, ramping from room temperature to 600 °C at 4 °C/min under a 500 mL/min N_2 gas flow. Approximately 14 mg of sample was briefly loaded into an open Al_2O_3 crucible in air before being purged with N_2.

Temperature programmed desorption (TPD-MS) was performed on a PCT-Pro E&E (Hy-Energy) coupled to a quadrupole mass spectrometer (MS) residual gas analyzer (Stanford Research Systems RGA 300). For each measurement, ~30 mg of sample was outgassed at 3×10^{-7} bar and 25 °C for >12 h. While still under dynamic vacuum, the samples were heated at 2 °C/minute, and after heating the samples were then allowed to cool to room temperature. TPD under hydrogen backpressure was performed at the same heating rate into a large calibrated volume.

Fourier transform infrared (FTIR) spectra were collected using a Bruker IFS 66 FT-IR with 64 background and 64 sample scans, co-averaged, and ratioed. A water-cooled globar source and a room-temperature deuterated trigylcine sulfate detector were used. The spectrometer was purged with dry nitrogen. Samples were prepared by encapsulation within pressed KBr pellets.

3. RESULTS AND DISCUSSION

3.1. Synthesis and Dehydration of $Li_2B_{12}H_{12}{\cdot}xH_2O$. The lithium salt $Li_2B_{12}H_{12}{\cdot}xH_2O$ was prepared by treatment of $(Et_3NH)_2(B_{12}H_{12})$ with lithium hydroxide following a modification of the literature procedure.[35] An excess of lithium hydroxide was added to a suspension of $(Et_3NH)_2(B_{12}H_{12})$ in water. The resulting solution was evaporated to dryness under a stream of nitrogen to remove triethylamine. The residue was dissolved in water and treated with the weak acid cation exchange resin Amberlite IRC86 in the H^+ form to neutralize and remove the excess lithium hydroxide. Filtration and evaporation afforded the hydrate $Li_2B_{12}H_{12}{\cdot}xH_2O$. The ^1H and ^{11}B NMR spectra for D_2O solutions of the salt were consistent with those reported for $M_2(B_{12}H_{12})$ (M = Na, K, Cs) (see Figures S1 and S2).[36] In addition to the broad signal in the ^1H NMR spectrum at ca. 0.5−1.8 ppm, which is a result of the $B_{12}H_{12}^{2-}$ anion, the spectrum also displays minor sharp signals at ca. 1.2 and 3.2 ppm that are consistent with the presence of $B_{12}H_{11}(NEt_2)^-$, at a level of ca. 3% (based on ^1H NMR). The impurity can form during the synthesis of the $B_{12}H_{12}^{2-}$ anion when following the decaborane/triethylamine-borane procedure.[37] The XRD data presented in Figure 1 also demonstrates the high purity of the as-synthesized $Li_2B_{12}H_{12}{\cdot}xH_2O$. The two known hydrates of $Li_2B_{12}H_{12}$ ($4H_2O$[38] and $7H_2O$[39]) are both present. Similar synthesis methodologies are utilized in previous $Li_2B_{12}H_{12}$ studies.[22,23]

Only a single previous study has reported on the dehydration properties of $Li_2B_{12}H_{12}{\cdot}xH_2O$ up to 250 °C.[39] DTA/TGA data for $Li_2B_{12}H_{12}{\cdot}xH_2O$ are presented in Figure 2 up to 600 °C. The previous study[39] revealed that water evolves from the structure in two distinct steps, from each of the hydrated structures. A slow thermal ramp rate was used (1 °C/min) in this earlier study, resulting in dehydration at 56 and 151 °C. We observe the same dual-step mechanism of dehydration below 200 °C with a faster thermal ramp (4 °C/min).

Of particular interest is the endothermic event at 350 °C that occurs before any H loss is observed. This signal is typically representative of a phase change or melting event. To clarify the nature of the 350 °C endothermic event, $Li_2B_{12}H_{12}$ was heated to both 350 and 375 °C at 4 °C/min and quenched back to room temperature. XRD data of the recovered material revealed that no change in structure had occurred in the 350 °C sample (see Figure 5). A very weak halo could be observed in the 375 °C sample, which becomes significantly more intense

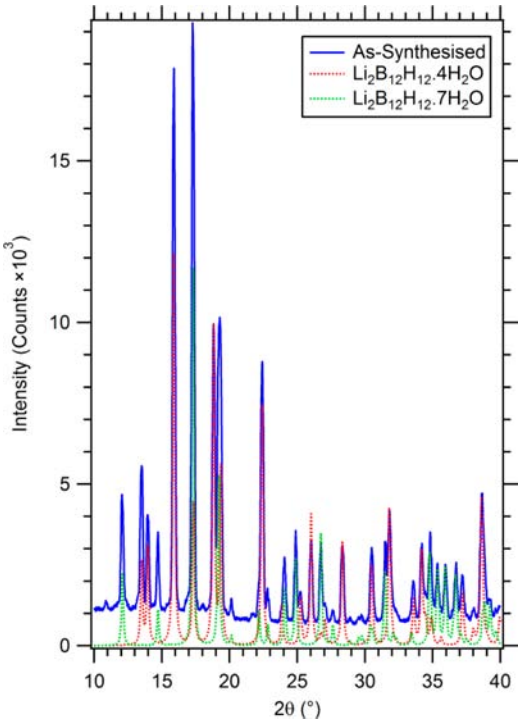

Figure 1. XRD patterns for wet chemically synthesized $Li_2B_{12}H_{12}{\cdot}xH_2O$.

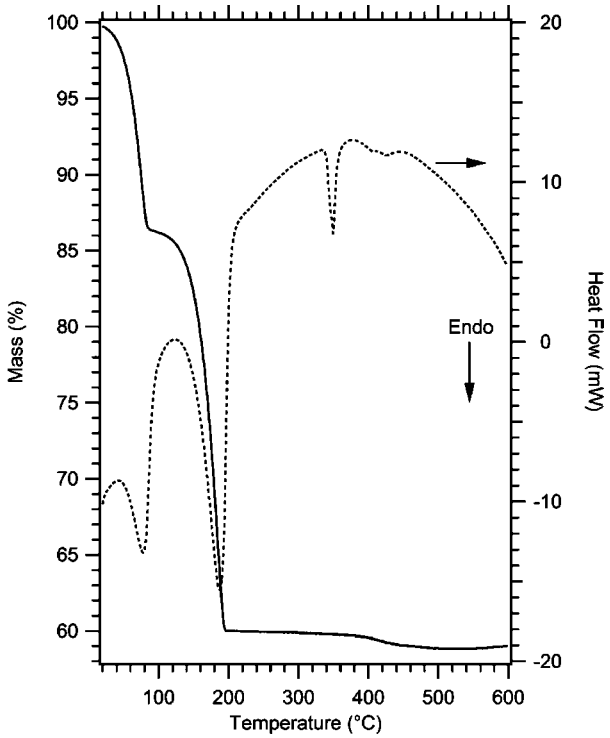

Figure 2. DTA/TGA data from $Li_2B_{12}H_{12}{\cdot}xH_2O$ heated at 4 °C/min under flowing N_2. The dotted black line represents heat flow, while the solid line shows mass loss.

dx.doi.org/10.1021/ja400131b | J. Am. Chem. Soc. 2013, 135, 6930−6941

with temperature (see Figure 5 and discussion in Section 3.3). This suggests that if a complete polymorphic transition does occur at 350 °C, then it is only transient in nature, or fully reversible, similar to the submelting polymorphic reversible transition observed in $LiBH_4$.[40] An in situ diffraction study would need to be undertaken to verify the nature of the structural modification of $Li_2B_{12}H_{12}$. No melting/fusion/frothing of the $Li_2B_{12}H_{12}$ was observed, and well-powdered material was recovered.

The endothermic peak at 350 °C for $Li_2B_{12}H_{12}$ has been observed previously[41] in the thermal ramping of $Li_2B_{12}H_{12}{\cdot}7NH_3$ where it was associated with a phase change. However, this study reported[41] that a new crystalline phase was observed in XRD after ramping, but it was not identified. Further investigation reveals that the reported XRD pattern appears similar to lithium silicate, possibly due to the fact that thermal ramping was performed in quartz crucibles that may react with the sample at temperature. Adverse reactions between similar compounds ($LiBH_4$) and SiO_2 are well-known.[13,42]

Further endothermic events are detected around 380−440 °C that are coupled with a noticeable mass loss. The release of hydrogen from closo-dodecaborane structures has been detected at relatively low temperatures for other species as well. DSC/TGA measurements undertaken on $K_2B_{12}H_{12}$[28] reveal a significant mass loss at ca. 355 °C, coupled with an endothermic spike and color change, indicative of a hydrogen desorption event. Another study[43] also demonstrates hydrogen desorption occurs from $Na_2B_{12}H_{12}$ at ca. 450 °C by TGA-MS.

Anhydrous $Li_2B_{12}H_{12}$ was synthesized through the dehydration of $Li_2B_{12}H_{12}{\cdot}xH_2O$ under flowing He at 225 °C for periods up to 6 h. TPD-MS of the water-laden $Li_2B_{12}H_{12}{\cdot}xH_2O$ hydrate, in Figure S3a, shows the majority of water is released by ca. 250 °C, with a third water evolution at ca. 300 °C that is associated with H release. This is in contrast to the case for water/H release from $MgB_{12}H_{12}{\cdot}xH_2O$ hydrate, where the majority of H is released simultaneously with water evolution, and in this case anhydrous $MgB_{12}H_{12}$ cannot be obtained from the hydrated structure.[21] As discussed in the $MgB_{12}H_{12}{\cdot}xH_2O$ study,[21] "$Mg(H_2O)_6B_{12}H_{12}.6H_2O$ has different thermal decomposition behavior from that of most hydrated alkali and alkaline earth salts of dodecahydrodecaborates".

In the same manner as earlier studies,[22,23] isothermal dehydration was implemented to obtain anhydrous $Li_2B_{12}H_{12}$. After 1 h of isothermal dehydration of $Li_2B_{12}H_{12}{\cdot}xH_2O$ at 225 °C, subsequent TPD-MS, in Figure S3b, reveals that a minor amount of water evolution can still be observed. XRD analysis of the 1 h dehydrated sample revealed 95.5 mol % anhydrous crystalline $Li_2B_{12}H_{12}$, with ca. 4.5 mol % $Li_2B_{12}H_{12}{\cdot}xH_2O$ remaining, indicating 0.8% oxygen atoms remain in the sample. After 6 h of isothermal dehydration of $Li_2B_{12}H_{12}{\cdot}xH_2O$ at 225 °C, the subsequent TPD-MS, in Figure S3c, shows an absence of a water signal, indicating complete dehydration. Even after 6 h of isothermal dehydration of $Li_2B_{12}H_{12}{\cdot}xH_2O$ at 225 °C, XRD data still indicated ca. 4.5 mol % $Li_2B_{12}H_{12}{\cdot}xH_2O$ remaining (see Figure 3), which is inconsistent with the absence of a water signal in the TPD-MS. Subsequent studies revealed that the dehydrated anhydrous crystalline $Li_2B_{12}H_{12}$ was absorbing water from the atmosphere through the sealed 300 nm Al foil during XRD measurements. This motivated us to study the hygroscopic nature of anhydrous $Li_2B_{12}H_{12}$, as described below in Section 3.2. We note that the dehydration period has not been specified in previous $Li_2B_{12}H_{12}$ studies.[22,23]

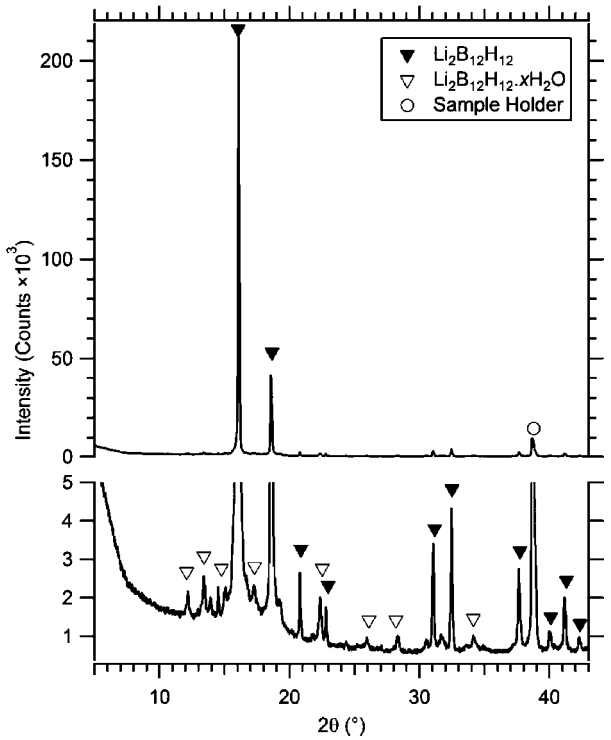

Figure 3. XRD pattern for anhydrous crystalline $Li_2B_{12}H_{12}$ after 6 h of isothermal dehydration at 225 °C. The zoomed background in the bottom caption shows the minor amount of $Li_2B_{12}H_{12}{\cdot}xH_2O$ (<4.5 mol %) grown during XRD measurement.

However, the XRD data reported for the structural solution of anhydrous crystalline *Pa*-3 $Li_2B_{12}H_{12}$ does not display any reflections from hydrate, as it has been sealed in a glass capillary under inert atmosphere.[22]

3.2. Deliquescence of $Li_2B_{12}H_{12}$. $Li_2B_{12}H_{12}$ is known to be extremely hygroscopic[22] and as such requires handling in an inert dry atmosphere at all times. We have not found previous literature describing the process of $Li_2B_{12}H_{12}{\cdot}xH_2O$ hydrate formation from anhydrous $Li_2B_{12}H_{12}$. During a 1 h XRD measurement, we observe the growth of ca. 4.5 mol % $Li_2B_{12}H_{12}{\cdot}xH_2O$ on completely anhydrous crystalline $Li_2B_{12}H_{12}$. The absorption of water most likely occurred through micropores in the 300 nm Al foil we use to cover and protect the sample from air. As such, we performed experiments by leaving the sample protected under the Al foil in atmosphere with 55% relative humidity. After a further 4 h of exposure, the original anhydrous $Li_2B_{12}H_{12}$ has been completely converted to crystalline $Li_2B_{12}H_{12}{\cdot}xH_2O$ hydrate. The hydrate contains a $4H_2O$[38] and $7H_2O$[39] mixture, with ca. 70 mol % of $Li_2B_{12}H_{12}{\cdot}7H_2O$, as shown in Figure 4b. Further exposure leads to complete liquefication of the hydrate, or deliquescence. Figure 4c shows the XRD pattern from the dissolved salt solution. Figure S4 shows the process of deliquescence occurring rapidly on a 10 min time scale when the sample is directly exposed to atmosphere. A study of the group II $MB_{12}H_{12}$ salts (M = Ca, Sr, Ba) demonstrates the process of hydration is completely reversible.[44] It has also been noted in the synthesis of $Li_2B_{12}H_{12}{\cdot}7H_2O$ for structure solution that the crystals are deliquescent.[39]

3.3. Decomposition of Anhydrous Crystalline $Li_2B_{12}H_{12}$. In order to determine the thermal stability and related mass loss from anhydrous $Li_2B_{12}H_{12}$ a TPD-MS

dx.doi.org/10.1021/ja400131b | J. Am. Chem. Soc. 2013, 135, 6930−6941

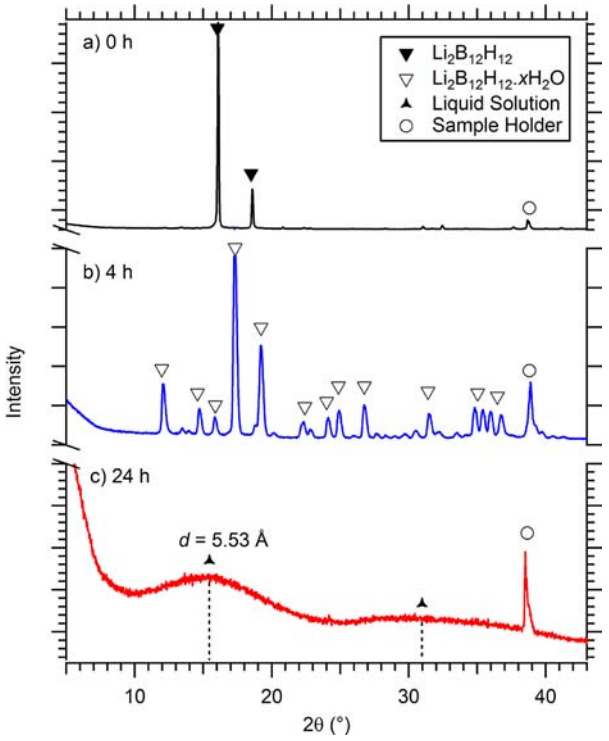

Figure 4. Deliquescence of anhydrous $Li_2B_{12}H_{12}$ at room temperature over 24 h.

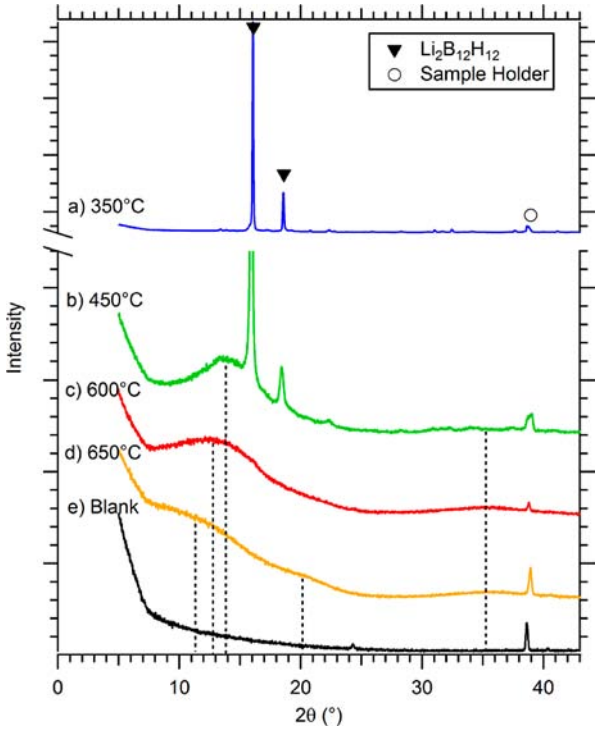

Figure 5. XRD data from thermally decomposed anhydrous crystalline $Li_2B_{12}H_{12}$ before and after the main H evolution peak at ca. 440 °C.

measurement was undertaken to detect which gases were released as a function of temperature (see Figure S3c and Figure 8). For all the following decomposition studies (hydrogen release) of $Li_2B_{12}H_{12}$, completely anhydrous crystalline $Li_2B_{12}H_{12}$ was used by isothermally decomposing $Li_2B_{12}H_{12}\cdot xH_2O$ for 6 h at 225 °C. The most relevant finding is the significant release of hydrogen after ca. 250 °C, with maxima at ca. 440 °C. This correlates well with the ca. 380−440 °C mass loss step (ca. 1.85 H atoms) in the DTA/TGA measurements in Figure 2. No MS signal from water or diborane could be discerned. To follow the decomposition of $Li_2B_{12}H_{12}$, we have measured samples heated to 350, 450, 600, and 650 °C, as shown in Figure 5a−d.

At 350 °C, before the onset of the main H evolution peak we observe by TPD-MS, the sample remains as crystalline $Li_2B_{12}H_{12}$, shown in Figure 5a. At 450 °C, after the major H evolution, we observe a two-phase pattern in Figure 5b, with a minor proportion of crystalline *Pa*-3 $Li_2B_{12}H_{12}$ remaining in a diffraction pattern dominated by an intense and broad diffraction halo centered at a high *d*-spacing of ca. d = 6.35 Å. By 600 °C, all crystalline $Li_2B_{12}H_{12}$ is depleted, and only a broad halo remains at ca. d = 7.00 Å. This halo maximum is expanded by ca. 28% in *d*-spacing compared to the strongest diffracted intensity (111) from crystalline *Pa*-3 $Li_2B_{12}H_{12}$ at d = 5.49 Å. Commensurate with this expansion is the loss of at least 2 H atoms from the original $Li_2B_{12}H_{12}$ formula unit, according to our manometry. A second strong halo can be observed at d = 2.55 Å. After thermal decomposition to 600 °C, $Li_2B_{12}H_{12}$ powder changes color from white to a light-brown/pink color. Figure 5c shows there are no obvious sharp crystalline peaks. There is no evidence of LiH formation or any other known Li-containing phases in $Li_2B_{12}H_{12}$ decomposed to 600 °C. We note also that there is no difference in the XRD pattern obtained from $Li_2B_{12}H_{12}$ decomposed to 600 °C under vacuum or under a 10 bar H_2 backpressure, indicating that the equilibrium decomposition product of $Li_2B_{12}H_{12}$ is a $Li_2B_{12}H_{12-x}$ composition which diffracts with a broad primary halo at a higher *d*-spacing ca. d = 7.00 Å. By 650 °C, Figure 5d shows that the $Li_2B_{12}H_{12-x}$ halo has shifted to an even higher *d*-spacing and significantly decreased in intensity and that another halo can be observed diffracting at ca. d = 4.22 Å, consistent with the production of amorphous boron (*a*-B).[45] From 600 to 650 °C, there is a strong powder color change from pinkish/off-white to brown, also consistent with *a*-B being brown in color. There is still no LiH observable by 650 °C. Two possibilities exist for the lack of crystalline LiH: (i) Li will be continuously evolved from the sample, in a similar fashion to the high temperature loss of Cs from $Cs_2B_{12}H_{12}$.[27] We note that the vaporisation pressure of Li is ca. 10 Pa at 600 °C.[46] (ii) Li is retained within the decomposed $Li_2B_{12}H_{12-x}$ phase, which eventually transforms to *a*-B with Li dissolved in it, or *a*-$B_{1-x}Li_x$. We do not observe melting at any stage during heating to 650 °C, and the sample remains well powdered at all times. We note that the steady release of H from crystalline $Li_2B_{12}H_{12}$ is consistent with the movement of the intense halo to higher *d*-spacings, indicated by the dashed lines in Figure 5. This H-dependent shift in *d*-spacing mirrors the change in the ca. −15 ppm ^{11}B NMR chemical shift that can be observed in other studies.[23] We discuss the structural nature of this expanded $Li_2B_{12}H_{12-x}$ composition in Section 3.5.

3.4. Rehydrogenation of Partially Decomposed $Li_2B_{12}H_{12-x}$. It has been previously reported that "release of one H_2 molecule per $Li_2B_{12}H_{12}$ was observed" for "well-dehydrated" $Li_2B_{12}H_{12}$ and that "such transformation appears to require heating at temperatures above 450°C".[23] It is also noted in this study "the material became water insoluble at room temperature in contrast to high water solubility of neat $Li_2B_{12}H_{12}$". Our multiphase XRD data in Figure 5b support the

dx.doi.org/10.1021/ja400131b | J. Am. Chem. Soc. 2013, 135, 6930−6941

notion that temperatures >450 °C are required to completely modify the $Li_2B_{12}H_{12}$ crystal structure by way of H release. We also find that $Li_2B_{12}H_{12}$ decomposed to 600 °C is water insoluble and not deliquescent, indicative of a major phase change compared to the highly hygroscopic $Li_2B_{12}H_{12}$. A downfield movement of the ^{11}B NMR chemical shift from −15.6 to −12 ppm is reported for $Li_2B_{12}H_{12}$ decomposed to 450 °C.[23] This implies that the chemical shift may move further downfield with higher temperatures and further H loss, although it may be difficult to discern in solid-state ^{11}B NMR data due to the broad nature of the chemical shift. $Li_2B_{12}H_{12}$ decomposed to 450 °C has also been rehydrogenated at 450 °C/100 bar, and it is reported that the chemical shift moves upfield back to −15.6 ppm.[23] We note that the ^{11}B NMR data[23] appear very broad and likely multiphase at this temperature. Figure 6 shows diffraction data from the rehydrogenation (450 °C/125 bar) of anhydrous $Li_2B_{12}H_{12}$ samples first decomposed to 450 and 600 °C.

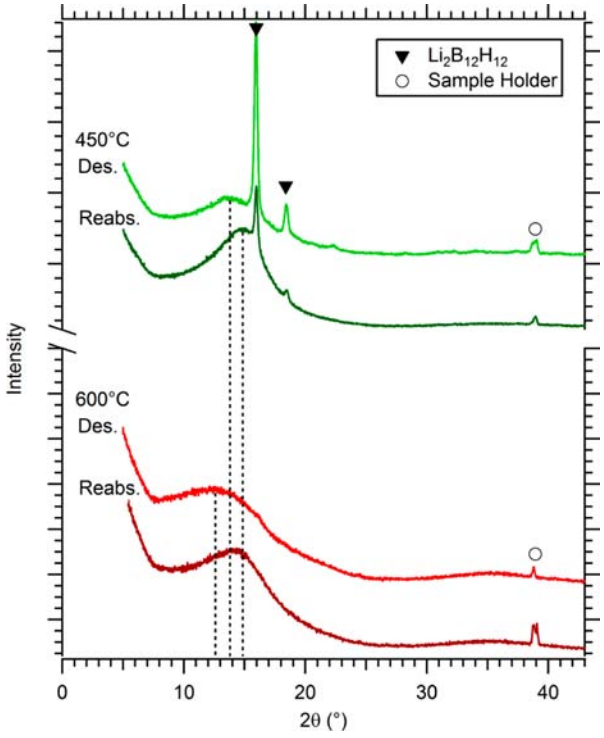

Figure 6. Rehydrogenation of $Li_2B_{12}H_{12}$ decomposed to 450 and 600 °C. Reabsorption of hydrogen occurred at 450 °C under 125 bar H_2 pressure.

After TPD to 450 °C, we observe a two-phase pattern composed of a broad diffraction halo at a *d*-spacing of ca. *d* = 6.35 Å, together with crystalline *Pa*-3 $Li_2B_{12}H_{12}$. After rehydrogenation at 450 °C/125 bar for 24 h, the crystalline $Li_2B_{12}H_{12}$ intensity is in fact strongly reduced, and the broad diffraction halo has significantly increased in intensity and shifted to a lower *d*-spacing of ca. *d* = 5.90 Å. Crystalline $Li_2B_{12}H_{12}$ decomposed to 600 °C only displays an intense diffraction halo at a *d*-spacing of ca. *d* = 7.00 Å, which after rehydrogenation at 450 °C/125 bar for 24 h shifts back to a lower *d*-spacing of ca. *d* = 5.90 Å. We note that release of H from $Li_2B_{12}H_{12}$ produces a diffraction halo which progressively shifts to higher *d*-spacings as more H is released and that the halo will shift back to lower *d*-spacings as H is reabsorbed. It is also notable that during rehydrogenation, the broad diffraction halo is favored over the regeneration of crystalline $Li_2B_{12}H_{12}$. Such diffraction features suggest that the ^{11}B NMR data displaying chemical shift movement from −12 to −15.6 ppm[23] during rehydrogenation (450 °C/100 bar) of decomposed $Li_2B_{12}H_{12}$ must be cautiously reinterpreted. The statement that "As expected, sharp peak at −15.6 ppm appears as a result of the recovery of $Li_2B_{12}H_{12}$" may not be accurate. The increase of the signal at −15.6 ppm for rehydrogenation (450 °C/100 bar) of decomposed $Li_2B_{12}H_{12}$[23] cannot be attributed to the recreation of crystalline *Pa*-3 $Li_2B_{12}H_{12}$, as crystalline *Pa*-3 $Li_2B_{12}H_{12}$ is clearly depleted during this process, as shown in Figure 6. Further understanding of this complex process is gained by inspection of Figure 7, which shows the instability of the known crystalline *Pa*-3 $Li_2B_{12}H_{12}$ structure[22] under *T*/*P* conditions far above the predicted H_2 equilibrium plateau.[32]

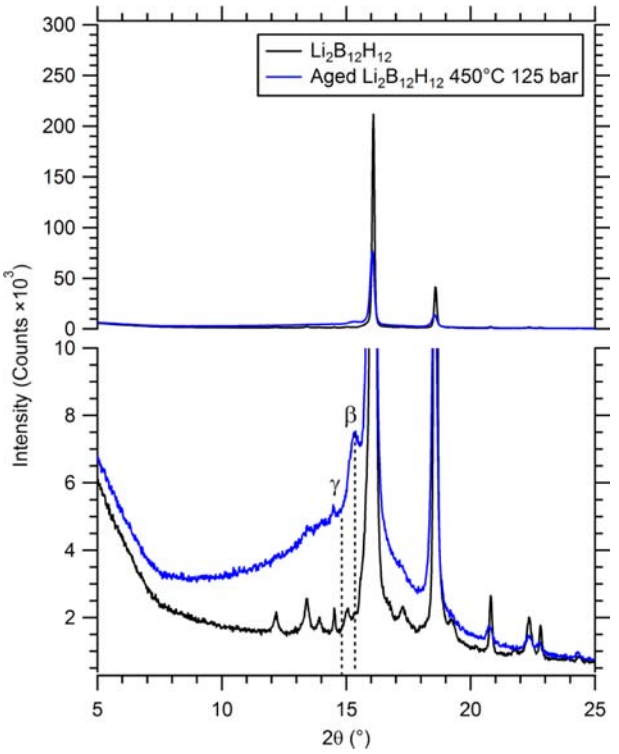

Figure 7. Anhydrous crystalline $Li_2B_{12}H_{12}$ aged at 450 °C and 125 bar H_2 pressure for 24 h.

Under the conditions of 450 °C and 125 bar H_2 pressure, anhydrous crystalline $Li_2B_{12}H_{12}$ is at a point in the equilibrium phase diagram that is ca. 17 000 times the predicted equilibrium plateau[32] for decomposition. Even though this prediction is for decomposition to B and not $Li_2B_{12}H_{12-x}$, it is to be expected that crystalline $Li_2B_{12}H_{12}$ would not release any H under such conditions. In Figure 7, we observe a remarkable feature: a moderately intense crystalline reflection at a *d*-spacing of ca. *d* = 5.76 Å can be observed on top of a broad diffraction halo centered at a *d*-spacing of ca. *d* = 5.85 Å. This small reflection appears as a high *d*-spacing satellite on the main *Pa*-3 $Li_2B_{12}H_{12}$ (111) reflection. As H release from $Li_2B_{12}H_{12}$ is highly unlikely under these *T*/*P* conditions, we believe we have detected two distinct polymorphic structures of $Li_2B_{12}H_{12}$, hereafter referred to as *β*-$Li_2B_{12}H_{12}$ (ca. *d* = 5.76 Å) and *γ*-$Li_2B_{12}H_{12}$ (ca. *d* = 5.85 Å). Presently it is not possible to discern if the crystalline

dx.doi.org/10.1021/ja400131b | J. Am. Chem. Soc. 2013, 135, 6930−6941

reflection at d = 5.76 Å has grown from a nanocrystalline state (represented by the broad halo underneath it at d = 5.85 Å) or if the crystalline β-$Li_2B_{12}H_{12}$ polymorph cannot sustain long-range order and collapses to a nanocrystalline γ-$Li_2B_{12}H_{12}$ modification, producing the broad diffraction halo underneath the crystalline reflection. Further in situ studies are required to discriminate the process. In either case, the d-spacing of ca. d = 5.85 Å marks the boundary of where the broad diffraction halo may be considered H full. Release of H under lower pressure conditions will shift the halo to higher d-spacings, as in Figure 6. Our observations suggest that the recovery of the −15.6 ppm chemical shift during rehydrogenation of decomposed $Li_2B_{12}H_{12}$[23] is attributable to nanocrystalline γ-$Li_2B_{12}H_{12}$, rather than the known Pa-3 $Li_2B_{12}H_{12}$ structure.[22] Solid-state ^{11}B chemical shifts below −15.6 ppm can then be attributed to the H-poor $Li_2B_{12}H_{12-x}$ composition. Further aging may increase the polymorphic proportion. We note that the position in d-spacing (ca. 5.90 Å) of the broad diffraction halos after rehydrogenation in Figure 6 is very close to the position of the broad halo from the $Li_2B_{12}H_{12}$ polymorph at ca. d = 5.85 Å in Figure 7, indicating nearly complete rehydrogenation. We emphasize that the existence of the β- and γ-$Li_2B_{12}H_{12}$ polymorphs must be further verified with a gravimetric study that accurately tests for a potential rise in H pressure during the aging period, which would indicate a phase weaker in H concentration. The very small mass of our samples in this study compared with manometer volumes presently precludes the confirmation of the polymorph. However, we note that the ca. d = 5.85 Å diffraction peak is at a similar position to the diffraction halo (ca. 5.90 Å) in rehydrogenated $Li_2B_{12}H_{12}$, suggesting the presence of a hydrogen full γ-$Li_2B_{12}H_{12}$ polymorph.

3.5. Decomposition of $LiBH_4$. Our results are of particular importance when considering the decomposition mechanism of $LiBH_4$. Figure 8 compares the TPD-MS of $LiBH_4$ with $Li_2B_{12}H_{12}$. $LiBH_4$ melts at ca. 280 °C[15] and typically does not begin releasing hydrogen until >330 °C even under vacuum conditions.[1,47] It has long been speculated that the major boron-containing decomposition product of $LiBH_4$ was $Li_2B_{12}H_{12}$ due to its reported significant stability[7] and spectroscopic indications, such as Raman[3,11] and ^{11}B NMR.[16] However, $Li_2B_{12}H_{12}$ clearly decomposes in a similar temperature range to $LiBH_4$.

3.5.1. Equilibrium Decomposition of $LiBH_4$. Only a single previous study[5] reports XRD data after traversing the $LiBH_4$ equilibrium plateau at temperatures >T_m. A broad low-angle halo can be observed in this XRD data, however, it was not discussed. We have traversed a $LiBH_4$ equilibrium isotherm at 500 °C, releasing pressure stepwise from 20 to 1 bar. Figure 9 compares the XRD data from this isothermally decomposed $LiBH_4$ sample with decomposed $Li_2B_{12}H_{12}$.

The isothermally decomposed $LiBH_4$ sample displays an intense diffraction halo at a high d-spacing of ca. 7.00 Å as well as sharp LiH reflections. We note that $LiBH_4$ that has been isothermally decomposed at 500 °C to 1 bar H_2 pressure produces an identical broad diffraction halo to decomposed $Li_2B_{12}H_{12}$, providing the first direct evidence by XRD that a substoichiometric $Li_2B_{12}H_{12-x}$ composition forms during the $LiBH_4$ decomposition process, which in structural terms is a new phase, strongly expanded from the unadulterated crystalline Pa-3 $Li_2B_{12}H_{12}$ unit cell. This is supported by weight and intensity standard quantification with a known weight fraction of LaB_6 added to the decomposed $LiBH_4$, which reproduces the expected 1:6 Li:B ratio for the unknown fraction of the sample compared to the observed LiH fraction. Until this study, no weight quantification had been carried out to quantify the amount of LiH that forms during $LiBH_4$

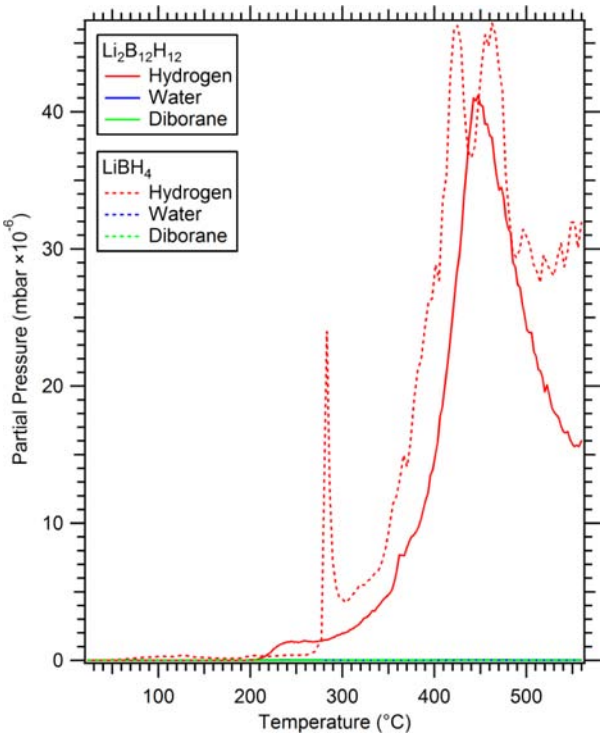

Figure 8. TPD-MS spectra from 6 h dehydrated $Li_2B_{12}H_{12}$. The sample was heated at 2 °C/minute under dynamic vacuum. $LiBH_4$ (Sigma-Aldrich) is shown for comparison.

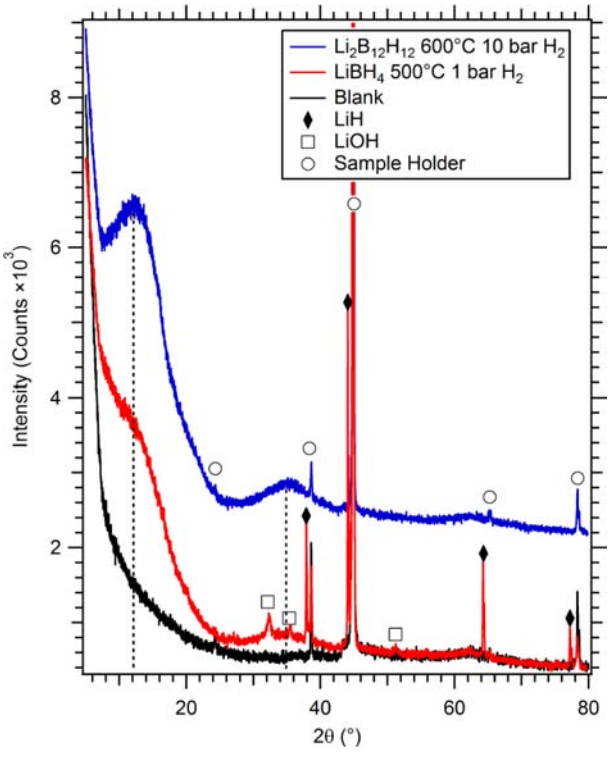

Figure 9. XRD data from $Li_2B_{12}H_{12}$ and $LiBH_4$ after thermal decomposition up to 600 °C.

dx.doi.org/10.1021/ja400131b | J. Am. Chem. Soc. 2013, 135, 6930−6941

decomposition. We also note that our diffraction data for isothermally decomposed $LiBH_4$ appear similar to the only previous XRD study.[5] The $Li_2B_{12}H_{12-x}$ halo in decomposed $LiBH_4$ is weaker in intensity compared to the single phase $Li_2B_{12}H_{12-x}$ halo, as it constitutes only ca. 9 mol % of the sample in decomposed $LiBH_4$.

As has been the case for solid-state ^{11}B NMR indicating the formation of a $Li_2B_{12}H_{12}$ intermediate during $LiBH_4$ decomposition, Raman data have also presented with typical B−H stretches at ca. 2500 cm^{-1} that indicate the formation of a $Li_2B_{12}H_{12}$-type phase. Figure 10 presents FTIR data for

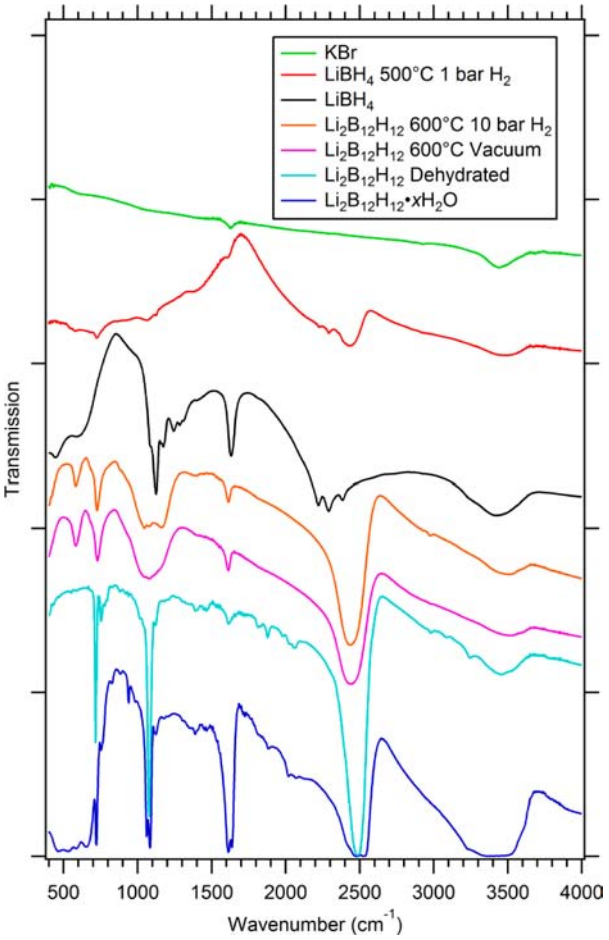

Figure 10. FTIR spectra for unadulterated and decomposed $LiBH_4$ and $Li_2B_{12}H_{12}$ samples.

decomposed $LiBH_4$ and $Li_2B_{12}H_{12}$ samples which display prominent B−H stretching modes clustered within a broad feature at ca. 2500 cm^{-1}, similar to previous studies.[3,11] The FTIR spectrum from decomposed $Li_2B_{12}H_{12}$ retains the three prominent bands at ca. 715, 1080, and 2480 cm^{-1}, however, a new mode can be observed in decomposed $Li_2B_{12}H_{12}$ at ca. 580 cm^{-1} which does not appear in unadulterated single-phase $Li_2B_{12}H_{12}$. This mode has been incorrectly assigned as originating from the $Li_2B_{12}H_{12}$ structure in previously reported Raman spectra.[3,7] The presence of this mode indicates a change in the original $Li_2B_{12}H_{12}$ structure, which can be correlated with the recent report of H mass loss from thermally decomposed $Li_2B_{12}H_{12}$,[23] consistent with our TPD-MS data in Figure 8. The 580 cm^{-1} band also appears in decomposed $LiBH_4$ in our FTIR data. It is notable that the 580 cm^{-1} band appears in amorphous $BH_{0.25}$ compositions,[48] but its structural origins are presently not clear.

We note that −OH stretches at ca. 1600 and 3400 cm^{-1} are evident in the FTIR data for apparently anhydrous phases. It must be noted that KBr is hygroscopic (even when dehydrated). The KBr blank shows strong −OH stretching bands, that are of similar intensity to all $Li_2B_{12}H_{12}$ samples studied. It is presently not possible to unambiguously assign the proportion of the −OH stretch that is induced from environmental contamination, although it is clearly the majority of the −OH signal. Based on our TPD-MS for dehydrated $Li_2B_{12}H_{12}$, we believe the phase is highly pure, ≫95%. Commercially obtained $LiBH_4$ quotes similar purity levels. Even so, it is possible that minor amounts of oxygen remain in the samples, <1%. Notably, a minor amount of LiOH is evident in the decomposed $LiBH_4$, suggesting the commercial powder retains a minor amount of oxygen.

Of particular relevance to the proposed decomposition mechanism of $LiBH_4$ is the original solid-state ^{11}B NMR study proposing the formation of crystalline $Li_2B_{12}H_{12}$ in $LiBH_4$ samples decomposed under H_2 backpressure.[16] It is notable that these ^{11}B NMR data appear identical to the ^{11}B NMR data for decomposed $LiBH_4$ in later studies,[23] with the broad ^{11}B NMR signal centered at ca. −12 ppm. Further, in the original study,[16] the ^{11}B NMR peak for decomposed $LiBH_4$ is clearly offset from a $K_2B_{12}H_{12}$ standard by ca. 3 ppm. This ca. 3 ppm offset is clearly discussed and related to loss of 2 H atoms from crystalline $Li_2B_{12}H_{12}$,[23] and as discussed above in Section 3.4, and shown in Figure 5, loss of H from crystalline $Li_2B_{12}H_{12}$ results in the formation of a new substoichiometric $Li_2B_{12}H_{12-x}$ phase which diffracts with a broad halo at *d*-spacings of 5.85−7.00 Å. The exact position of the halo in *d*-spacing is dependent on the amount of H released, as shown in Figure 6. Our XRD data strongly support the notion that the original solid-state ^{11}B NMR study[16] has in fact identified the substoichiometric $Li_2B_{12}H_{12-x}$ phase. The thermodynamic model for $LiBH_4$ decomposition presented in the most recent ^{11}B NMR study,[7] also containing broad chemical shifts centered at −12 ppm, should be reassessed on the basis of our findings.

At 500 °C and 1 bar system pressure in the equilibrium-phase diagram, decomposed $LiBH_4$ samples are almost completely depleted of hydrogen.[5] We have quenched samples from a lower temperature of 480 °C, from approximately the middle of the equilibrium plateau, yielding a sample comprised of undecomposed $LiBH_4$ (recrystallized on cooling), LiH, and a broad diffraction halo from $Li_2B_{12}H_{12-x}$ at ca. d = 5.85 Å, shown in Figure 11b. Under these conditions the $Li_2B_{12}H_{12-x}$ halo exists at a *d*-spacing consistent with the H full state in Figures 6 and 7. This suggests that initially, $LiBH_4$ decomposes to H full γ-$Li_2B_{12}H_{12}$ and LiH and that the H full γ-$Li_2B_{12}H_{12}$ subsequently decomposes to $Li_2B_{12}H_{12-x}$. We discuss the complete decomposition mechanism below in Section 3.5.2.

We note that the most recent ^{11}B NMR study of decomposed $LiBH_4$ samples[7] utilizes XRD data to a low enough angle to observe the diffraction halo from substoichiometric $Li_2B_{12}H_{12-x}$ but that glassy capillaries are used which significantly attenuate and mask the low-angle portion of the pattern and perturb the background over a wide angular range. It is specifically for this reason that thin crystalline film be used in Debye−Scherrer geometry (i.e., Al in this study) or crystalline sapphire capillaries in transmission geometry.

3.5.2. Vacuum Decomposition of $LiBH_4$. It has been stated since the earliest studies on the thermography of $LiBH_4$[49] that

dx.doi.org/10.1021/ja400131b | J. Am. Chem. Soc. 2013, 135, 6930−6941

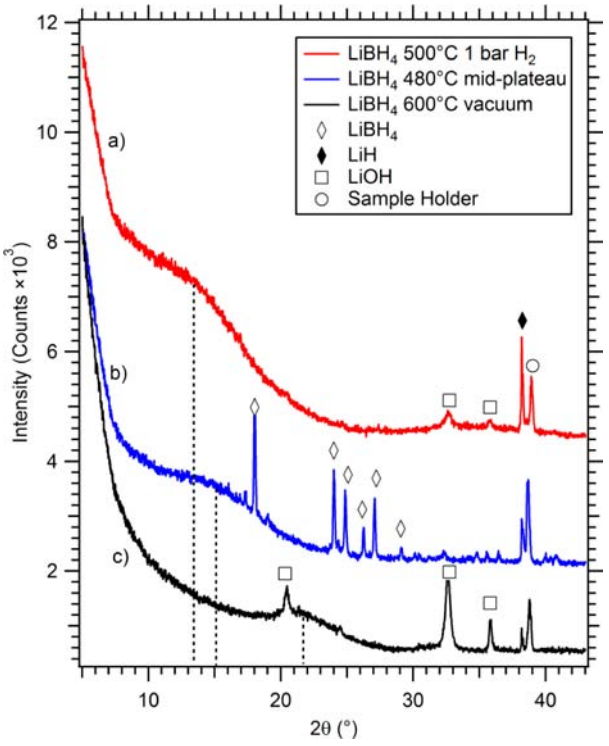

Figure 11. XRD data from $LiBH_4$ after isothermal decomposition under various pressure and temperature conditions.

the decomposition reaction should be $LiBH_4 \rightarrow LiH + B$, which will yield a maximum H release of 13.13 wt % H. Surprisingly, there exists no structural evidence to support this mechanism. While XRD data from decomposed $LiBH_4$ samples can display crystalline LiH reflections,[2−5] no diffraction evidence exists for the presence of crystalline or amorphous boron, which diffracts with a strong primary and secondary halo at d = 4.22 and 2.55 Å, respectively.[50] Even with the use of quartz (or glassy) capillaries, which can overlap with the primary amorphous boron halo, the secondary amorphous boron halo at d = 2.55 Å is still strong and obvious, yet is not observable in any of the reported XRD data.[2−5] Despite this, amorphous boron is regularly reported to exist on the basis of ^{11}B NMR data in $LiBH_4$ decomposed under low pressure (0.1 bar)/vacuum conditions, in the 500−600 °C temperature range.[7,16] It is notable that amorphous boron standards are typically contaminated with oxygen[50] and require high-temperature treatment to remove the oxygen and purify the boron. As such, without supporting XRD data unequivocally showing the primary and secondary amorphous boron halo and an oxygen free phase, the assignment of amorphous boron as a broad feature centered at ca. 0 ppm in solid-state ^{11}B NMR data from decomposed $LiBH_4$ is presently ambiguous.

Also problematic with the structural interpretation of $LiBH_4$ samples decomposed under vacuum or low-H backpressure is the behavior of the molten $LiBH_4$ phase. We observe that the melt can easily climb sample cell walls over ca. 5 cm distances and that filters can be plugged up to a distance of 30 cm from the sample. We note that the Li vaporisation pressure at 600 °C is ca. 10 Pa.[46] The ability of vaporous $LiBH_4$ to deposit products on cell walls has also been observed previously.[51] We typically observe such problems at temperatures $>T_m$ under vacuum conditions. See Supporting Information and Figure S6 for further discussion related to the complex multiphase decomposed $LiBH_4$ samples that form when cell filters are plugged. Further confusing the exact mechanism of $LiBH_4$ decomposition under vacuum conditions is in situ Raman data collected under flowing Ar (i.e., zero H_2 backpressure), where the formation of $Li_2B_{12}H_{12}$ (including the misassigned peak at 580 cm^{-1} which is not present in pure $Li_2B_{12}H_{12}$) and amorphous boron is proposed.[20] On the basis of observing the 580 cm^{-1} band in our study of decomposed $Li_2B_{12}H_{12}$, this in situ Raman study in fact suggests that the substochiometric $Li_2B_{12}H_{12-x}$ composition has formed.

Figure 11c shows XRD data for $LiBH_4$ decomposed to 600 °C under vacuum, continuously monitored by MS. During the entire desorption period (ca. 5 h), we observed only a hydrogen signal, with no diborane, water, or oxygen signal evident. However, a significant quantity (larger than that observed in Figure 9) of LiOH has formed in the sample. The only other phases we observe are LiH and a broad halo at ca. d = 4.02 Å, corresponding closely to a-B. No $Li_2B_{12}H_{12-x}$ halo can be observed. This suggests that the sample has been completely dehydrogenated but has sustained oxygen contamination during the process. We observe shiny black crystals from the bottom of the cell and flaky cream-colored crystals higher up on the cell walls, indicating melt climbing. The flaky crystals are composed only of a halo corresponding to $Li_2B_{12}H_{12-x}$ and LiH (similar pattern to Figure 11a), indicating this part of the melt climbed from the hot zone of the furnace and did not completely desorb. Such an inhomogeneous sample composition is not unexpected considering the above discussion about melt climbing/sample frothing/Li vapor loss under vacuum conditions. LiOH is present in decomposed $LiBH_4$ due to the purity of the starting reagent. However, in this case, the LiOH has been concentrated at the base of the cell, along with the well-decomposed $LiBH_4$, phase segregated from a larger portion of partially decomposed $LiBH_4$. It should be noted that this LiOH has recrystallized from its melting point of ca. 462 °C.

Despite the presence of impurities, we have demonstrated that the substoichiometric $Li_2B_{12}H_{12-x}$ composition will eventually release all hydrogen. The position of the a-B halo is at ca. d = 4.02 Å and is compressed in d-spacing compared to its expected position of ca. 4.22−4.40 Å.[50,52] This compression in d-spacing of the a-B halo is consistent with Li remaining within it, and we note, for example, the study of 12 at % Mg dissolved into a-B[53] and similar studies of Zr and V.[54] Due to the phase segregation, it is presently not possible to quantify by weight standard the expected amount of LiH if all Li from the $Li_2B_{12}H_{12-x}$ phase remains with the B, in the order of 16.7 at %, a similar quantity to that observed for Mg.[53] We also note that while the solubility of Li in a-B has previously been stated as negligible,[55] the production of a-$B_{1-x}Li_x$ has never been conceived as being possible from $LiBH_4$ decomposition. The halo for a-B in $Li_2B_{12}H_{12}$ decomposed to 650 °C (see Figure 5) does not display a d-spacing contraction and exists at ca. d = 4.22 Å. This suggests the presence of LiH may be responsible for the production of a-$B_{1-x}Li_x$ in decomposed $LiBH_4$. Based on the reinterpretation of existing solid-state ^{11}B NMR data[7,16,23] and our diffraction analysis above, the complete decomposition sequence of $LiBH_4$ may be written as three distinct steps:

$$12LiBH_4 \rightarrow \gamma\text{-}Li_2B_{12}H_{12} + 10LiH + 13H_2$$

$$\gamma\text{-}Li_2B_{12}H_{12} + 10LiH \rightarrow Li_2B_{12}H_{12-x} + 10LiH + x/2H_2$$

dx.doi.org/10.1021/ja400131b | J. Am. Chem. Soc. 2013, 135, 6930−6941

$$Li_2B_{12}H_{12-x} + 10LiH \rightarrow (12)a\text{-}BLi_{(y+2)/12} + (10 - y)LiH + (12 - x + y)/2H_2$$

The total wt % H released is dependent on the amount of Li remaining in a-$B_{1-x}Li_x$. We note that the first two steps are dependent on gravimetric confirmation of the γ-$Li_2B_{12}H_{12}$ polymorph being hydrogen full, and while we allow for the possibility of direct decomposition to $Li_2B_{12}H_{12-x}$, the halo position at ca. d = 5.85 Å strongly suggests a hydrogen full γ-$Li_2B_{12}H_{12}$ polymorph. Reported H loss from $LiBH_4$ is variable, in the range 10.9−13.8 wt % H (note that 13.1 wt % H is the theoretical maximum H release according to $LiBH_4 \rightarrow LiH + B$). Pure $LiBH_4$ desorbs 9 wt % H to 600 °C under its own evolved backpressure,[1] and 13.8 wt % H is released under flowing He to 600 °C, with only weak LiH peaks observable in XRD data.[3] A full 3 H atoms are claimed to be released under vacuum to 727 °C, however, many crystalline reflections other than LiH are evident in XRD data[4] (suggesting vapor blocking), and 10.9 wt % H is released isothermally under flowing H_2 up to 517 °C, with the formation of a broad and intense halo which was not recognized or discussed.[5] As this is the only previous study identifying similar samples to this study, we expect the composition reached is $Li_2B_{12}H_{7.4}$ based on the reported H release. In light of the Li loss/molten sample frothing/climbing container walls we observe during $LiBH_4$ decomposition under low pressure conditions, reported losses of H to >10 wt % H up to 600 °C must be qualified with supporting XRD weight standard quantification of the amount of Li left in the sample. We note, for example, that melt frothing/bubbling/spitting/Li vapor loss etc. from DTA/TGA crucibles will give an artifactual overestimate of wt % H released.

Discussion of the decomposition mechanism of $LiBH_4$ is not complete without the consideration of diborane (B_2H_6) as a potential controlling mechanism. As discussed comprehensively in our study of $Mg(BH_4)_2$ decomposition, when decomposed tetravalent borohydrides are placed in water, they bubble violently and produce diborane.[15] During this process of dissolution, metal-$B_{12}H_{12}$ phases are artifactually produced from the reaction of diborane with the original unreacted tetravalent complex hydride. The same process has been observed in the solid-state reaction of B_2H_6 with $LiBH_4$ at 200 °C, producing crystalline $Li_2B_{12}H_{12}$ and apparently amorphous $Li_2B_{10}H_{10}$.[56] We note that this reaction temperature of 200 °C is considerably lower than T_m for $LiBH_4$ where H release begins. In our study, we do not observe a MS signal from diborane (or decomposition fragments) during any of our decompositions of either $LiBH_4$ or $Li_2B_{12}H_{12}$. This is consistent with the MS study which indicates diborane emissions from pure $LiBH_4$ decomposition exist only at trace/impurity levels (even less under H_2 backpressure).[57] We note also that the major H release event from $LiBH_4$ is >300 °C, above the dissociation temperature for diborane,[58] and none of the diborane decomposition products (boranes)[58] have been observed in ^{11}B NMR data. Presently, the role of diborane in pure $LiBH_4$ decomposition appears physically unlikely at temperatures $>T_m$.

It is notable that it is not necessary to completely dehydrogenate $LiBH_4$ until a-$B_{1-x}Li_x$ production occurs. Rehydrogenation of $LiBH_4$ has been successful from $Li_2B_{12}H_{12-x}$ and LiH, under 600 °C/350 bar.[5] Similarly, ball-milled mixtures of $Li_2B_{12}H_{12}$ + LiH have been partially rehydrogenated to $LiBH_4$ at 500 °C/900 bar.[59] It is preferable to preserve the remaining 2−3 wt % H in the $Li_2B_{12}H_{12-x}$ phase and avoid sample segregation under vacuum conditions.

3.5.3. Structural Properties of Polymorphic β- and γ-$Li_2B_{12}H_{12}$ and Decomposed $Li_2B_{12}H_{12-x}$. The structure of the β-$Li_2B_{12}H_{12}$ polymorph is at least transiently crystalline, as shown in Figure 7. Aside from the strongest crystalline reflection at ca. d = 5.76 Å, there exists no other obvious reflections with which to index the unit cell symmetry. It is notable that a more stable (by ca. 7 kJ/mol) monoclinic $C2/m$ structure type has been predicted for $Li_2B_{12}H_{12}$,[32] which gives strongest calculated intensity (111) at ca. d = 5.90 Å. This is at the same position at which we observe the halo from γ-$Li_2B_{12}H_{12}$, as in Figures 6 and 7. Further in situ aging experiments are necessary to grow more of both β and γ phases to clarify their structure type.

The partially hydrogen decomposed $Li_2B_{12}H_{12-x}$ phase is related to the nanocrystalline γ-$Li_2B_{12}H_{12}$ polymorph, as shown in Figure 7, and may possess the same symmetry as the parent γ-$Li_2B_{12}H_{12}$ structure. With such broad diffraction halos, the structure of the expanded $Li_2B_{12}H_{12-x}$ phase presently cannot be determined independently by wide angle XRD alone. The fact that the solid state ^{11}B NMR chemical shift remains in the vicinity of −12 to −15.6 ppm for decomposed $Li_2B_{12}H_{12}$ with no new chemical shift observable[23] suggests that the B_{12} icosahedral cage environment remains for $Li_2B_{12}H_{12-x}$. The broad width of the ca. d = 7.00 Å diffraction halo for $Li_2B_{12}H_{12-x}$ suggests the phase is either amorphous or nanocrystalline in nature. An amorphous $Li_2B_{12}H_{12-x}$ composition is unlikely from the perspective that the XRD pattern would likely diffract at considerably lower d-spacing, similar to Li dissolved in a-B, which would diffract with a primary halo in the vicinity of ca. 4.2−4.4 Å (see Figure S5 and further discussion in Supporting Information). We also note that a broadened crystalline $Li_2B_{12}H_{12}$ model diffraction pattern appears quite similar (albeit shifted to lower d-spacings) to decomposed $Li_2B_{12}H_{12-x}$ XRD data, and we expect the $Li_2B_{12}H_{12-x}$ phase retains a high unit cell symmetry, while the phase exists in nanoparticulate/nanocrystalline form. The sharp LiH reflections compared to the broad $Li_2B_{12}H_{12-x}$ diffraction halos (in decomposed $LiBH_4$) indicate that boron segregation has occurred. Due to the fact that $LiBH_4$ can be regenerated from similarly decomposed samples,[5] it is likely that as crystallization occurs from the molten $LiBH_4$ phase during decomposition, the correct 1:1 Li:B proportion is retained in individual crystallized powder grains. It has been postulated that polymerization of $Li_2B_{12}H_{12}$ units/adducts should occur on the basis of mass loss of at least 2 H atoms and downfield shift of signals from −15.6 to −12 ppm in solid-state ^{11}B data.[7,23] However, our FTIR data indicate otherwise, with no observable B−H−B bridging bands occurring for >1000 cm^{-1}, such as we observe for decomposed $Mg(BH_4)_2$.[15] As such, we expect that the H poor $B_{12}H_{12-x}$ icosahedra remain isolated for the $Li_2B_{12}H_{12-x}$ phase. Face sharing/fusing of B_{12} icosahedra during polymerization would also produce new ^{11}B chemical shifts, which are not observed. Recent density functional theory modeling indicates the possibility of stable neutral and anionic $Li_2B_{12}H_{10}$ compositions with 2 H atoms removed,[60] which may be representative of the early stages of γ-$Li_2B_{12}H_{12}$ decomposition. On this basis, to retain isolated H poor $B_{12}H_{12-x}$ icosahedra in an expanded unit cell suggests that the Li atoms adopt a new coordination around the isolated H poor $B_{12}H_{12-x}$ icosahedra. An example of one such coordination is P−P

dx.doi.org/10.1021/ja400131b | J. Am. Chem. Soc. 2013, 135, 6930−6941

dipoles in $B_{12}P_2$,[61] suggesting the original isolated Li atoms may recoordinate as Li−Li dipoles to expand the unit cell. Total scattering studies and precession electron diffraction[62] may elucidate these crystallographic details.

4. CONCLUSIONS

Since the pioneering synthesis work of Stock[63] on boranes and Schlesinger[42] on metal-borohydrides, there is collectively over 150 years of research into boron-based materials with H in their structure. While these materials have been widely used in solution chemistry, surprisingly few structural studies exist concerning the mechanism of H release during thermally induced solid−gas reactions. For example, the solid−gas B−H phase diagram is currently unknown.[64] We report the synthesis of anhydrous crystalline $Li_2B_{12}H_{12}$ and demonstrate that it is highly sensitive to the absorption of water from ambient atmosphere, identifying the structural mechanism by which deliquescence of $Li_2B_{12}H_{12}{\cdot}xH_2O$ crystals occur. Concerning the release of H from single-phase anhydrous crystalline $Li_2B_{12}H_{12}$, the implications of our study are compelling: for $LiBH_4$, the proposed formation of crystalline $Li_2B_{12}H_{12}$ (*Pa*-3 structure type)[22] during thermal decomposition is not apparent, and a new γ-$Li_2B_{12}H_{12}$ polymorph is observed to be the intermediate decomposition product of $LiBH_4$. Our XRD, TPD-MS, and FTIR data and analysis provide evidence that $LiBH_4$ decomposes via a previously unobserved γ-$Li_2B_{12}H_{12}$ polymorph directly to a substoichiometric $Li_2B_{12}H_{12-x}$ composition, diffracting with a broad peak in the *d*-spacing range 5.85−7.00 Å, dependent on the quantity of H released. Previous literature reporting solid-state ^{11}B NMR data are entirely consistent with this H poor $Li_2B_{12}H_{12-x}$ composition at −12 ppm. Solid-state ^{11}B NMR data in the range −12 to −15 ppm indicate that H poor $B_{12}H_{12-x}$ motifs retain a pseudoicosahedral environment. FTIR spectra of $Li_2B_{12}H_{12-x}$ report vibrational frequencies very similar to B−H bonds in unadulterated $Li_2B_{12}H_{12}$. The lack of a B−H−B bridging band at >1000 cm^{-1} indicates that H poor $B_{12}H_{12-x}$ icosahedra do not polymerize and remain isolated, with an, as yet, undetermined charge. We have also observed the complete dehydrogenation of $LiBH_4$ to a-$B_{1-x}Li_x$ and LiH. All thermodynamic models[7,32] related to $LiBH_4$ decomposition must be reassessed on the basis of the γ-$Li_2B_{12}H_{12}$ polymorph, and that the $Li_2B_{12}H_{12-x}$ phase can exist with variable H concentration. We note that all theoretical models display van't Hoff lines that are of significantly different gradient[65] to experimentally determined van't Hoff data.[5] Solid-state ^{11}B NMR, Raman/FTIR, quantitative XRD, and quantitative H desorption measurements should all be used in a combinatorial fashion to elucidate metal-borohydride decomposition mechanisms. $Li_2B_{12}H_{12}$ displays considerable polymorphism, and further structural studies are required to elucidate the symmetry of all $Li_2B_{12}H_{12}$ polymorphs.

■ ASSOCIATED CONTENT

Supporting Information

^1H and ^{11}B NMR spectra for $Li_2B_{12}H_{12}{\cdot}xH_2O$, and TPD-MS and XRD data showing ball-milled $Li_2B_{12}H_{12}$ and $LiBH_4$ samples formed artifactually from Li vapor plugging cell filters and photographs of the process of deliquescence. This material is available free of charge via the Internet at http://pubs.acs.org.

■ AUTHOR INFORMATION

Corresponding Author

mark.pitt@gmail.com

Notes

The authors declare no competing financial interest.

■ ACKNOWLEDGMENTS

The authors would like to thank A. Rossiter at FETI, Curtin University for her assistance with DTA/TGA measurements. We acknowledge the facilities, scientific, and technical assistance with FTIR measurements of P. Chapman, Department of Chemistry, Curtin University. C.E.B., M.P., and D.A.S. acknowledge the financial support of the Australian Research Council for ARC Linkage grant LP120100435, and C.E.B. acknowledges the ARC for ARC LIEF grants LE0775551 and LE0989180. D.H.B. acknowledges the support of Curtin University for a Curtin University Research and Teaching Fellowship.

■ REFERENCES

(1) Zuttel, A.; Rentsch, S.; Fischer, P.; Wenger, P.; Sudan, P.; Mauron, P.; Emmenegger, C. *J. Alloys Compd.* **2003**, *356−357*, 515.
(2) Orimo, S.; Nakamori, Y.; Kitahara, G.; Miwa, K.; Ohba, N.; Towata, S.; Zuttel, A. *J. Alloys Compd.* **2005**, *404−406*, 427.
(3) Orimo, S.; Nakamori, Y.; Ohba, N.; Miwa, K.; Aoki, M.; Towata, S.; Zuttel, A. *Appl. Phys. Lett.* **2006**, *89*, 021920.
(4) Zuttel, A.; Borgschulte, A.; Orimo, S. *Scr. Mater.* **2007**, *56*, 823.
(5) Mauron, P.; Buchter, F.; Friedrichs, O.; Remhof, A.; Bielmann, M.; Zwicky, C. N.; Zuttel, A. *J. Phys. Chem. B* **2008**, *112*, 906.
(6) Chen, R.; Wang, X.; Xu, L.; Li, H.; Chen, C.; Chen, L.; Pan, H. *J. Alloys Compd.* **2011**, *509*, 3481.
(7) Yan, Y.; Remhof, A.; Hwang, S.-.; Li, H.-.; Mauron, P.; Orimo, S.; Zuttel, A. *Phys. Chem. Chem. Phys.* **2012**, *14*, 6514.
(8) Severa, G.; Ronnebro, E.; Jensen, C. M. *Chem. Commun.* **2010**, *46*, 421.
(9) Newhouse, R. J.; Stavila, V.; Hwang, S.-J.; Klebanoff, L. E.; Zhang, J. Z. *J. Phys. Chem. C* **2010**, *114*, 5224.
(10) Pitt, M. P.; Webb, C. J.; Paskevicius, M.; Sheptyakov, D.; Buckley, C. E.; Gray, E. M. *J. Phys. Chem. C* **2011**, *115*, 22669.
(11) Reed, D.; Book, D. *Mater. Res. Soc. Symp. Proc.* **2010**, *1216*, W06.
(12) Martelli, P.; Remhof, A.; Borgschulte, A.; Mauron, P.; Wallacher, D.; Kemner, E.; Russina, M.; Pendolino, F.; Zuttel, A. *J. Phys. Chem. A* **2010**, *114*, 10117.
(13) Mosegaard, L.; Moller, B.; Jorgensen, J.-E.; Filinchuk, Y.; Cerenius, Y.; Hanson, J. C.; Dimasi, E.; Besenbacher, F.; Jensen, T. R. *J. Phys. Chem. C* **2008**, *112*, 1299.
(14) Pitt, M. P.; Vullum, P. E.; Sørby, M. H.; Emerich, H.; Paskevicius, M.; Buckley, C. E.; Walmsley, J. C.; Holmestad, R.; Hauback, B. C. *J. Phys. Chem. C* **2012**, *116*, 14205.
(15) Paskevicius, M.; Pitt, M. P.; Webb, C. J.; Sheppard, D. A.; Filsø, U.; Gray, E. M.; Buckley, C. E. *J. Phys. Chem. C* **2012**, *116*, 15231.
(16) Hwang, S.-J.; Bowman, R. C.; Reiter, J. W.; Rijssenbeek; Soloveichik, G. L.; Zhao, J.-C.; Kabbour, H.; Ahn, C. C. *J. Phys. Chem. C* **2008**, *112*, 3164.
(17) Soloveichik, G. L.; Gao, Y.; Rijssenbeek, J.; Andrus, M.; Kniajanski, S.; Bowman, R. C., Jr; Hwang, S.-J.; Zhao, J.-C. *Int. J. Hydrogen Energy* **2009**, *34*, 916.
(18) Li, H. W.; Kikuchi, K.; Nakamori, Y.; Ohba, N.; Miwa, K.; Towata, S.; Orimo, S. *Acta Mater.* **2008**, *56*, 1342.
(19) Li, H. W.; Miwa, K.; Ohba, N.; Fujita, T.; Sato, T.; Yan, Y.; Towata, S.; Chen, M. W.; Orimo, S. *Nanotechnology* **2009**, *20*, 204013.
(20) Reed, D.; Book, D. *Mater. Res. Soc. Symp. Proc.* **2010**, *1216*, 172.
(21) Chen, X.; Lingam, H. K.; Huang, Z.; Yisgedu, T.; Zhao, J.-C.; Shore, S. G. *J. Phys. Chem. Lett.* **2010**, *1*, 201.

(22) Her, J.-H.; Yousufuddin, M.; Zhou, W.; Jalisatgi, S. S.; Kulleck, J. G.; Zan, J. A.; Hwang, S.-J.; Bowman, R. C., Jr.; Udovic, T. J. *Inorg. Chem.* **2008**, *47*, 9757.
(23) Hwang, S.; Bowman, R. C.; Kim, C.; Zan, J. A.; Reiter, J. W. *J. Anal. Sci. Technol.* **2011**, *2*, A159.
(24) Kuznetsov, N. T.; Klimchuk, G. S. *Russ. J. Inorg. Chem.* **1971**, *16*, 645.
(25) Muetterties, E. L.; Balthis, J. H.; Chia, Y. T.; Knoth, W. H.; Miller, H. C. *Inorg. Chem.* **1964**, *3*, 444.
(26) Isaenko, L. I.; Myakishev, K. G.; POsnaya, I. S.; Volkov, V. V. *Izv. Sib. Otd. Akad. Nauk SSSR, Ser. Khim. Nauk* **1982**, *2*, 73.
(27) Tiritiris, I. PhD Thesis. Universität Stuttgart: Stuttgart, Germany, 2003.
(28) Kaste, P. *Studies of the effect of hivelite and other boron compounds on nitramine decomposition by pyrolysis GC-FTIR*, ADA206802 (BRL-TR-2973); U.S. Army Ballistic Research Laboratory: Adelphi, MD, 1988.
(29) Solntsev, K. A.; Kuznetsov, N. T.; Ponomarev, V. I. *Dokl. Chem.* **1976**, *228*, 391.
(30) Schroeder, M. A. *Borohydride Catalysis of Nitramine Thermal Decomposition and Combustion: III. Literature Review and Wrap-up Discussion of Possible Chemical Mechanisms*, ADA224918 (BRL-TR-3126); U.S. Army Ballistic Research Laboratory: Adelphi, MD, 1990.
(31) Stavila, V.; Her, J.-H.; Zhou, W.; Hwang, S.-J.; Kim, C.; Ottley, L. A. M.; Udovic, T. J. *J. Solid State Chem.* **2010**, *183*, 1133.
(32) Ozolins, V.; Majzoub, E. H.; Wolverton, C. *J. Am. Chem. Soc.* **2009**, *131*, 230.
(33) Caputo, R.; Zuttel, A. *Mol. Phys.* **2010**, *108*, 1263.
(34) Miller, H. C.; Muetterties, E. L.; Boone, J. L.; Garrett, P.; Hawthorne, M. F. *Inorg. Synth.* **1968**, *10*, 81.
(35) Johnson, J. W.; Brody, J. F. *J. Electrochem. Soc.* **1982**, *129*, 2213.
(36) Geis, V.; Guttsche, K.; Knapp, C.; Scherer, H.; Uzun, R. *Dalton Trans.* **2009**, 2687.
(37) Miller, H. C.; Miller, N. E.; Muetterties, E. L. *Inorg. Chem.* **1964**, *3*, 1456.
(38) Yousufuddin, M.; Her, J.-H.; Zhou, W.; Jalisatgi, S. S.; Udovic, T. J. *Inorg. Chim. Acta* **2009**, *362*, 3155.
(39) Tiritiris, I.; Schleid, T. *Z. Anorg. Allg. Chem.* **2002**, *628*, 1411.
(40) Filinchuk, Y.; Chernyshov, D.; Cerny, R. *J. Phys. Chem. C* **2008**, *112*, 10579.
(41) Huang, Z.; Gallucci, J.; Chen, X.; Yisgedu, T.; Lingam, H. K.; Shore, S. G.; Zhao, J.-C. *J. Mater. Chem.* **2010**, *20*, 2743.
(42) Schlesinger, H. I.; Brown, H. C. *J. Am. Chem. Soc.* **1940**, *62*, 3429.
(43) Caputo, R.; Garroni, S.; Olid, D.; Teixidor, F.; Surinach, S.; Baro, M. D. *Phys. Chem. Chem. Phys.* **2010**, *12*, 15093.
(44) Solntsev, K. A.; Kuznetsov, N. T.; Kol'ba, L. N.; Agre, V. M.; Ponomarev, V. I. *Russ. J. Inorg. Chem.* **1977**, *22*, 171.
(45) Jiang, J.; Senkowicz, B. J.; Larbalestier, D. C.; Hellstrom, E. E. *Supercond. Sci. Technol.* **2006**, *19*, L33.
(46) Davison, H. W. *Compilation of Thermophysical Properties of Liquid Lithium; Nasa Technical Note, TN D-4650*; NASA: Washington, D.C., 1968.
(47) Luo, C.; Wang, H.; Sun, T.; Zhu, M. *Int. J. Hydrogen Energy* **2012**, *37*, 13446.
(48) Wang, P.; Orimo, S.; Tanabe, K.; Fujii, H. *J. Alloys Compd.* **2003**, *350*, 218.
(49) Stasinevich, D. S.; Egorenko, G. A. *Russ. J. Inorg. Chem.* **1968**, *13*, 341.
(50) Jiang, J.; et al. *Supercond. Sci. Technol.* **2006**, *19*, L33.
(51) Toyoda, H.; Watanabe, M.; Sugai, H. *J. Nucl. Mater.* **1997**, *241*−*243*, 1031.
(52) Gillespie, J. S. *J. Am. Chem. Soc.* **1966**, *88*, 2423.
(53) Kim, H.-M.; Yim, S.-S.; Kim, K.-B.; Kang, D.-H.; Moon, S.-H.; Kim, Y.-W.; Lee, H.-N. *J. Mater. Res.* **2004**, *19*, 409.
(54) Tanabe, K.; Soga, K.; Hosoi, S.; Osumi, K.; Yamaguchi, H.; Uruga, T.; Kimura, K. *J. Phys. Soc. Jpn.* **2011**, *80*, 024709.
(55) Borgstedt, H. B. *J. Phase Equilib.* **2003**, *24*, 572.
(56) Friedrichs, O.; Remhof, A.; Hwang, S.-J.; Zuttel, A. *Chem. Mater.* **2010**, *22*, 3265.
(57) Borgschulte, A.; Callini, E.; Probst, B.; Jain, A.; Kato, S.; Friedrichs, O.; Remhof, A.; Bielmann, M.; Ramirez-Cuesta, A. J.; Zuttel, A. *J. Phys. Chem. C* **2011**, *115*, 17220.
(58) Soderlund, M.; Maki-Arvela, P.; Eranen, K.; Salmi, T.; Rahkola, R.; Murzin, D. Y. *Catal. Lett.* **2005**, *105*, 191.
(59) Udovic, T. J.; Kattner, U. R. 2010 DOE Vehicle Technologies and Hydrogen Programs Annual Merit Review and Peer Evaluation Meeting, Washington, D.C., June 7−10, 2010; Department of Energy: Washington, D.C.; http://www.hydrogen.energy.gov/pdfs/review10/st067_udovic_2010_p_web.pdf.
(60) Pancharatna, P. D.; Balakrishnarajan, M. M.; Jemmis, E. D.; Hoffmann, R. *J. Am. Chem. Soc.* **2012**, *134*, 5916.
(61) Emin, D. *J. Solid State Chem.* **2006**, *179*, 2791.
(62) Hadermann, J.; Abakumov, A.; Rompaey, S. V.; Perkisas, T.; Filinchuk, Y.; Tendeloo, G. V. *Chem. Mater.* **2012**, *24*, 3401.
(63) Stock, A. *Hydrides of Boron and Silicon*; Cornell University Press: Ithaca, NY, 1933.
(64) Predel, B. B−Ba ... Cu−Zr. *Landolt-Börnstein - Group IV Physical Chemistry*; Springer-Verlag: Berlin, Germany, 2012; Vol *12B*, p 46.
(65) Kharbachi, A. E.; Pinatel, E.; Nuta, I.; Baricco, M. *CALPHAD: Comput. Coupling Phase Diagrams Thermochem.* **2012**, *39*, 80.